

A MULTICORE BASED PARALLEL IMAGE REGISTRATION METHOD

Lin Yang^{§‡}, Leiguang Gong[†], Hong Zhang^{§‡}, John L. Noshier[‡], and David J. Foran^{§‡}

[§]Center of Biomedical Imaging and Informatics, The Cancer Institute of New Jersey,
UMDNJ-Robert Wood Johnson Medical School, Piscataway, NJ, 08854, USA

[†]IBM T. J. Watson Research, Hawthorne, NY, 10532, USA

[‡]Dept. of Radiology, UMDNJ-Robert Wood Johnson Medical School, Piscataway, NJ, 08854, USA

ABSTRACT

Image registration is a crucial step for many image-assisted clinical applications such as surgery planning and treatment evaluation. In this paper we proposed a landmark based nonlinear image registration algorithm for matching 2D image pairs. The algorithm was shown to be effective and robust under conditions of large deformations. In landmark based registration, the most important step is establishing the correspondence among the selected landmark points. This usually requires an extensive search which is often computationally expensive. We introduced a nonregular data partition algorithm using the K -means clustering algorithm to group the landmarks based on the number of available processing cores. The step optimizes the memory usage and data transfer. We have tested our method using IBM Cell Broadband Engine (Cell/B.E.) platform.

1. INTRODUCTION

Image registration is the process of determining the linear or nonlinear mapping between two images of the same object or similar objects acquired at different time, or from different perspectives. Given two images taken at different time (usually one is referred to as fixed image and the other is the moving image), the problem can be described as finding a linear or nonlinear transformation which maps each point in the fixed image to a point in the moving image. For nonlinear registration, some of methods describe the transformation based on elastic deformations, such as fluid deformation based algorithm [1, 2] and Demon's algorithm [3, 4]. The others model the transformation by a function with some parameters, such as B-spline based image registration algorithm [5].

Both intensity and landmark based methods have been reported to be effective in managing various registration tasks. Hybrid methods which integrate both strategies are also proposed for fully automatic registration applications [6, 7, 8]. Point matching in medical images is particularly challenging due to the variability introduced by image acquisition and the variation of the anatomical structures. Automatic algorithms for landmark detection and matching have been developed

[6, 7], though the robustness of those methods has not been sufficiently demonstrated.

We introduce an alternative landmark point detection and matching method for performing the landmark based image registration for 2D images. The algorithm applies a Harris corner detector to find the landmarks and subsequently utilizes robust estimation to reject the outliers. It is fully automatic and unsupervised. The resulting landmark pairs are then used to estimate the nonlinear transformation T . We have developed a unique landmark based registration framework, which has proven to be effective in registering an image pair of large transformations or deformations.

In our proposed landmark based image registration algorithm, a major performance bottleneck was the landmark matching process since the algorithm relies on finding a large number of matching landmark points for accuracy. In this paper, we present a new accelerated parallel implementation of the landmark matching, which takes advantage of the *data independence* property of the algorithm. The parallel algorithm was implemented on the IBM Cell/B.E. multicore platform. The algorithm is very fast and can handle large transformation and deformation while still providing good registration results. The proposed image registration algorithm is described in Section 2. In Section 3, we describe a new non-uniform data partitioning and parallelization approach. The experimental results are presented in Section 4. Section 5 concludes the paper.

2. LANDMARK BASED IMAGE REGISTRATION

The image registration algorithm begins by automatically detecting a set of landmarks in both fixed and moving images, followed by a coarse to fine estimation of the nonlinear mapping using the landmarks. Robust estimation is used to find the robust correspondence between the landmarks in the fixed and moving image. The refined inliers are used to estimate a nonlinear transformation T and also deform the moving image to the fixed image.

The automatic landmark detection is the procedure used to accurately detect of the prominent and salient points in

the image. Harris corner detector was applied to find the points with the large gradients in both directions (x and y for 2D images). The original computation in the Harris corner detector involves the computation of eigenvalues. Instead, the determinant and trace are used to find the corners using $F = \det(A) - \alpha \text{trace}(A)$ where α is chosen as 0.1.

After we detect the landmarks, we can extract features from the neighborhood of each landmark. The local orientation histograms are used as the features for landmark matching. The image is first convolved with the orientation filters. The filtering response in the neighborhood around the landmarks is computed to compose the local orientation histogram. The local orientation histogram encodes the directions of the edges at each landmark point. It has proven to be an effective feature descriptor when the training samples are small [9].

In order to achieve robust matching of the landmarks, an extensive search in the image space and parameter space is required. This step is time consuming and often create the bottleneck for the landmark based image registration algorithm. In Section 3, we will show the time profile for each step in the whole procedure and clarify that the landmark matching step dominate the execution speed.

Because the original matching landmark sets contain missing landmarks, RANdom SAMple Consensus (RANSAC) [10] is used to reject outliers and robustly estimate the transformation. The RANSAC robust estimator randomly selects the minimal subset of the landmarks to fit the model. Measured by a cost function, the points within a small distance are considered as a consensus set. The size of the consensus set is called the model support M . The algorithm is repeated multiple times and the model exhibiting largest support is recorded as the robust fit. In Figure 1 we show the results of applying robust estimation to reject the outliers in the original matching landmarks. The Harris corner detector detected 32 landmark pairs in Figure 1b. Based on the assumption of an affine transformation, the RANSAC found 8 inliers (shown in Figure 1c) and the rest 24 matching landmarks are rejected as outliers under the assumption for an Affine transformation.

The thin plate spline transform (TPS) is used to estimate the nonlinear transformation between the fixed and moving image based on the robust landmark correspondence. The TPS transformation T is calculated by minimizing the bending energy. It can provide a smooth matching function for each point in both images. The resulting nonlinear transformation is applied to map the moving image to the fixed image. For more details, we refer readers to [11].

The adaptive multi-resolution landmark based image registration algorithm can provide good registration results, but requires relatively time consuming point matching procedures. In Figure 2 we show the execution time profile for each step in our algorithm for a typical 2D (192×192) image pair registration. It is quite obvious that the bottleneck is the point matching step. However, as mentioned previously, the

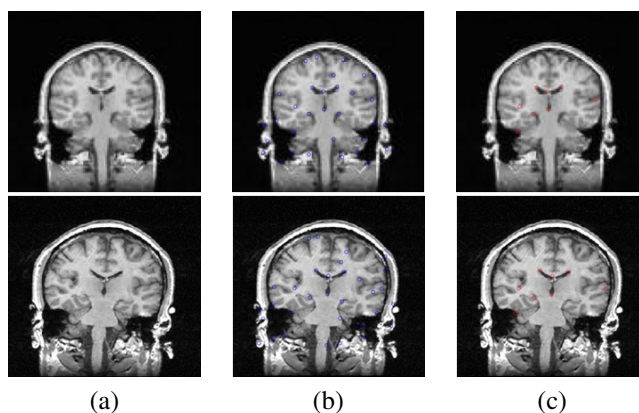


Fig. 1. Apply the robust estimation to find the robust landmark correspondence. (a)The original fixed and moving image. (b)The original pairs of matching points. (c)The robust matching points after rejecting the outliers.

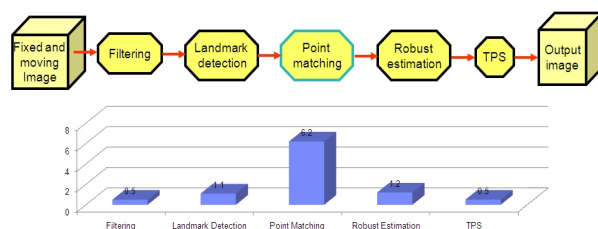


Fig. 2. The time profile for the entire nonlinear registration algorithm (seconds)

point matching procedure in the proposed algorithm offers a significant advantage for easy parallelization by its design: *data independence*. Each landmark in the fixed image is independent of all other landmarks, and its best match in the moving image is restricted to a certain size of moving image patch. By fully utilizing this property, we propose to apply K -means data partitioning approach, and it has been successfully implemented on the IBM Cell Broadband Engine processor.

3. PARALLELIZATION ON THE CELL/B.E.

The IBM Cell/B.E. [12] is a multicore chip with a relatively high number of cores. It contains a Power Processing Element (PPE) which has the similar function and configuration as the regular CPU. It also has multiple cores which are optimized for single precision float point algorithm, the Synergetic Processing Element (SPE). The PPE contains 32K L_1 cache, 512K L_2 cache and a large amount of physical memory (2G in our case). Unlike the PPE, the SPE has a quite different architecture compared with the standard CPU. The SPE operates on a 256KB local store to hold both the code and data. The SPE also support 128 bit Single Instruction, Multiple Data (SIMD) instruction set for effective vector opera-

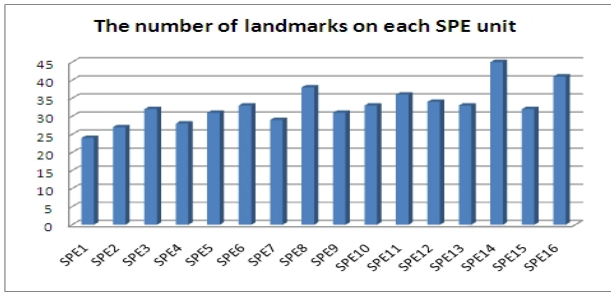


Fig. 3. The landmark distribution on each SPE unit of the IBM Cell/B.E.

tions. The data transfer between the SPE and PPE is through the direct memory access (DMA). DMA is quite time consuming therefore a good parallel implementation should minimize the number of DMA operations.

Given all the detected landmarks in the fixed image, we first apply the K -means algorithm to cluster them based on their Euclidean distance in the image, where $K = 16$ is set to be the number of the computing units in the IBM Cell Blade machine. Based on the boundary landmarks in each cluster center, we can calculate the largest and smallest coordinates to crop the sub-image accordingly. Because we know the size of the code running on the SPE unit in advance, we can compute the maximal size of the sub-image that can be stored on a single core (e.g. single SPE). If the image patch can fit into the local storage, the whole cluster of landmarks and their corresponding image patch are sent to the SPE for parallel processing using just one direct memory access (DMA). Because the number of DMA is critical for the performance of the parallel algorithm, the advantage of applying K -means to group the landmarks into clusters is to minimize the number of direct memory access operations. Landmarks which are spatially close to each other are grouped together and transferred into one computing core (e.g. one SPE in a Cell Processor) using one DMA call.

The purpose of applying K -means clustering for data partitioning is to decrease the number of direct memory access (DMA) operations. However, in order to fully utilize each SPE computing unit, the work load should be balanced. Because the algorithm selects the landmarks considering their spatial relationships, the K -means clustering intends to provide similar amount of landmarks in each cluster. In Figure 3 we show a typical work load distribution for one image pair on 16 SPE, it is clear that the number of landmarks assigned to each cluster roughly form a uniform distribution. The main processor or main core (e.g. PPE) is responsible for spooling and destroying all the threads of computing cores (e.g. SPE). It is also in charge of assembling all the matching points that returned from each SPE and converts the results back to the original image coordinate systems. Robust estimation is applied to reject outliers and preserve the robust landmark correspondence. Nonlinear transformation is finally estimated to

register the fixed image and the moving image.

4. EXPERIMENTAL RESULTS

The test data used in our experiments were prepared in the department of Radiology, University of Medicine and Dentistry of New Jersey. The dimensionality of the test image is 192×192 and the x and y resolution are 1.41 mm. We test our algorithm using the simulated affine transformations. Forty simulated 2D human abdomen CT images were generated by applying forty simulated deformations. The algorithm is compared with the multiple resolution affine registration implemented in ITK (<http://www.itk.org>) and also the free software MedINRIA developed by INRIA (<http://www-sop.inria.fr/asclepios/software/medinria/>). The registration accuracy is evaluated based on whether the algorithm can successfully recover the affine transformation parameters.

We define $E = \max \left\{ \frac{|p_t^* - p_t|}{\delta_t}, \frac{|p_r^* - p_r|}{\delta_r}, \frac{|p_s^* - p_s|}{\delta_s} \right\}$ where the p_t^*, p_r^*, p_s^* represent the estimated translation, rotation and scale parameters. The p_t, p_r, p_s are the ground true transformation parameters. The $\delta_t = 1, \delta_r = 0.5, \delta_s = 0.01$ are the normalization factors for translation, rotation and scale, respectively. The registration is considered successful if $E \leq 1.0$. Our proposed algorithm can recover 95% of the image pairs while the ITK and MedINRIA can only recover 70% and 50%, respectively, for image pairs with large deformation. From the experimental results we show that the proposed algorithm can accurately register two images under 2.5 times scale differences and 45 degrees of rotation. It is clear that our algorithm provides robust registration for large deformations when compared with the implementation in ITK and MedINRIA.

We also tested our algorithm using the CT scans from two different persons, and the imaged pathology specimens. We experimentally demonstrated that the algorithm can be applied to a wide range of medical image registration applications. Some experimental results are shown in Figure 4. The first row represents the fixed image. The second row is the moving image and results are shown in the third row. The registered images shown in the third row of Figure 4 are expected to be similar to the fixed images shown in the first row.

The parallelization code was compiled for two different platforms. The parallel version was running on an IBM BladeCenter Q21 featuring 2GB of RAM and two processors running at 3.2 GHz configured as a two-way, symmetric multiprocessor (SMP). A thread running on a PPE can communicate with all 16 SPEs. The Cell/B.E. SDK 3.0 and GCC compiler were used to implement and compile the algorithm. In all our experiments, there was one main thread running on one of the PPEs and up to 16 threads on the SPEs. The sequential version was running on a x86 machine at 2.6 GHz and 4G memory. The compiler is also GCC.

All the image pairs used for testing have dimensionality

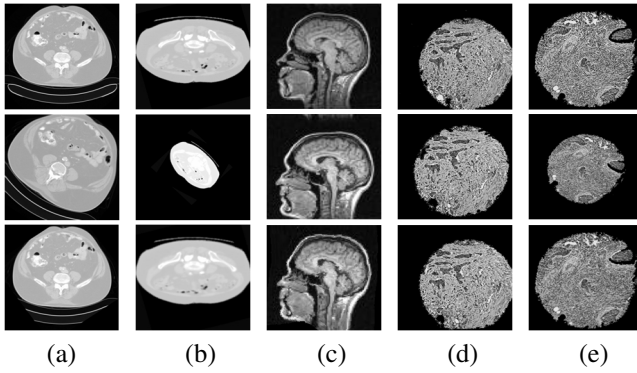


Fig. 4. The experimental results using different test image pairs. (a) and (b) The human abdomen CT image pair. (c) The MRI image of two different human head. (d) and (e) The imaged pathology specimens of human breast tissue.

Table 1. The comparative experiments of the point matching procedure using the sequential and parallel multicore platform (seconds)

	Mean	Variance	Median
x86	5.95	0.26	5.82
Cell/B.E. (PPE only)	6.13	0.001	6.12
Cell/B.E. (16 SPEs)	0.71	0.0032	0.70

(192×192). Because the point matching procedure dominates the running time of the registration algorithm, this step is the only part parallelized on the Cell/B.E. For fair comparison we run each implementation (sequential and parallel) 10 times. The comparative experiments of the running speed of the point matching procedure on two platforms are shown in Table 1. Please notice that x86 refers to the sequential implementation on a x86 machine running the Linux. The Cell/B.E. (PPE only) denotes the running time on the multicore processor using only the main processor PPE. The Cell/B.E. (16 SPEs) represents the parallel running time by fully utilizing all the 16 computing cores (SPEs). Using the multicore platform, we roughly achieved 10 times of speedup over its corresponding sequential implementation. In total, the parallel version of the algorithm can register a pair of image (192×192) in less than five seconds.

5. CONCLUSION

In this paper, we have explained a parallelization of a robust and accurate 2D image registration algorithm. The method is implemented on an IBM Cell/B.E. We have achieved approximately 10 fold speed up compared with its sequential implementation. Our proposed data partitioning approach and the parallelization schema are independent of the parallel platforms and are generic by design, therefore it can be extended to other applications on other parallel platforms.

6. ACKNOWLEDGEMENT

This research was primarily conducted in IBM Watson Research Center funded by its internship program. It is also supported in part, by grants from the NIH through contract 5R01EB003587-04 from the National Institute of Biomedical Imaging and Bioengineering and contract 5R01LM009239-02 from the National Library of Medicine. Additional support was provided by IBM through a Shared University Research Award.

7. REFERENCES

- [1] B. Cena, N. Fox, and J. Rees, "Fluid deformation of serial structural MRI for low-grade glioma growth analysis," in *MICCAI*, 2004, vol. 3217, pp. 1055–1063.
- [2] E. Agostino, F. Maes, D. Vandermeulen, and P. Suetens, "A viscous fluid model for multimodal non-rigid image registration using mutual information," *Medical Image Analysis*, vol. 7, no. 4, pp. 565–575, 2003.
- [3] J. P. Thirion, "Image matching as a diffusion process: An analogy with Maxwell demons," *Medical Image Analysis*, vol. 2, no. 3, pp. 243–260, 1998.
- [4] T. Vercauteren, X. Pennec, A. Perchant, and N. Ayache, "Non-parametric diffeomorphic image registration with the demons algorithm," in *MICCAI*, 2007, vol. 4792, pp. 319–326.
- [5] R. Szeliski, R. Szeliski, J. Coughlan, and J. Coughlan, "Hierarchical spline-based image registration," *International Journal of Computer Vision*, pp. 194–201, 1994.
- [6] C. DeLorenzo, X. Papademetris, K. Wu, K. P. Vives, D. Spencer, and J. S. Duncan, "Nonrigid 3D brain registration using intensity/feature information," *MICCAI*, vol. 4190, pp. 1611–3349, 2004.
- [7] B. Fischer and J. Modersitzki, "Combination of automatic and landmark based registration: the best of both worlds," *SPIE Medical Imaging*, pp. 1037–1047, 2003.
- [8] A. Azar, C. Xu, X. Pennec, and N. Ayache, "An interactive hybrid non-rigid registration framework for 3D medical images," *Proc. International Symposium on Biomedical Imaging*, pp. 824–827, 2006.
- [9] K. Levi and Y. Weiss, "Learning object detection from a small number of examples: the importance of good features," in *CVPR*, 2004, vol. 2, pp. 53–60.
- [10] M. A. Fischler and R. C. Bolles, "Random sample consensus: A paradigm for model fitting with applications to image analysis and automated cartography," *Comm. of the ACM*, vol. 24, pp. 381–395, 1981.
- [11] H. Chui and A. Rangarajan, "A new point matching algorithm for non-rigid registration," *Computer Vision and Image Understanding*, vol. 89, no. 2, pp. 114–141, 2003.
- [12] T. Chen, R. Raghavan, J. N. Dale, and E. Iwata, "Cell broadband engine architecture and its first implementation - A performance review," *IBM J. Res. Develop.*, vol. 51, no. 5, pp. 559–572, 2007.